

Effect of constitutive equations on theoretical analysis in melt spinning process

Seong Cheol Kim, Tae Hwan Oh*, Sung Soo Han and Won Seok Lyoo

School of Textiles, Yeung nam University, Kyeongsan 712-749, Korea

(Received May 20, 2009; final version received June 15, 2009)

Abstract

Profile development of the melt spinning process of poly(ethylene terephthalate) (PET) was simulated by a numerical method under the consideration of two constitutive equations of Newtonian and upper convected Maxwell (UCM) models. The viscoelastic characteristics of the polymer were considered *via* UCM constitutive equation that considered relaxation time as a function of temperature and molecular weight. The UCM model predicted the diameter profile better than the Newtonian, while velocity development was slower than the Newtonian model. Viscoelasticity played an important role in accurately predicting diameter profile. However, even though neck-like deformation was observed in the UCM model, the exact position of the deformation under high speed spinning was not obtained.

Keywords : profile development, numerical method, diameter profile, velocity profile

1. Introduction

Melt spinning is one of the polymer processes accompanying mass, momentum, and heat transfer. Not only physical and structural changes in melt spinning, but also melt spinning dynamics are the main focus of melt spinning research. The numerical method is a useful tool for analyzing melt spinning dynamics. Profile development such as velocity, temperature, stress, and diameter can be obtained *via* numerical simulation. The melt spinning process is mainly analyzed by employing the asymptotic method of thin filament equations, which formulate the dynamics of the spinning process averaging over a cross-section of filament (Kase and Matsuo, 1965; Denton *et al.*, 1995).

A Newtonian constitutive equation was used to simplify the sets of differential equations and reduce their nonlinearity. Most research centering upon numerical simulation in the spinning processes is carried out using Newtonian constitutive equation, under the assumption that the Newtonian model is reasonable in simulating the melt spinning process and is thus acceptable as a constitutive equation to simplify the governing equations to obtain converged solutions. However, the molten polymer used in melt spinning has shown non-Newtonian behavior. Shimizu *et al.* (1985) have used the Maxwell model with an assumption of a constant modulus while Kikutani *et al.* (1996) have used an upper convected Maxwell (UCM) model as a constitutive equation for simulating the dynamics of bicompo-

nent fiber spinning; however, the relaxation time was assumed to be constant.

In this work, the numerical simulation of poly(ethylene terephthalate) (PET) fiber spinning has been studied. In particular, the effect of the constitutive equation on profile development in melt spinning was investigated *via* a numerical method. Newtonian and upper convected Maxwell models were applied as constitutive equations with the relaxation time considered a function of temperature and molecular weight.

2. Formulation and Numerical Method

Fig. 1 shows a schematic of the melt spinning process. Governing equations of melt spinning dynamics are as follows. The steady state and incompressible melt flow were assumed (George, 1982; Cao *et al.*, 1989).

$$W = \rho A v_z \quad (1)$$

$$dF/dz = W(dv_z/dz - g/v_z) + \pi \rho_a v_z^2 C_f D/2 \quad (2)$$

$$dT/dz = -\pi Dh(T - T_a)/(WC_p) \quad (3)$$

where W represents the mass flow rate of polymer, A the area of fiber, v_z the axial velocity, ρ_a the density of air, F the force, z the position in axial direction, D the diameter, C_f the skin friction coefficient, g the gravity constant, C_p the specific heat capacity of polymer, h the heat transfer coefficient of polymer, T the temperature of polymer, and T_a the temperature of surrounding air.

Newtonian fluid as a constitutive equation is as follows

$$F = \eta A (dv_z/dz), \quad (4)$$

*Corresponding author: taehwanoh@ynu.ac.kr
© 2009 by The Korean Society of Rheology

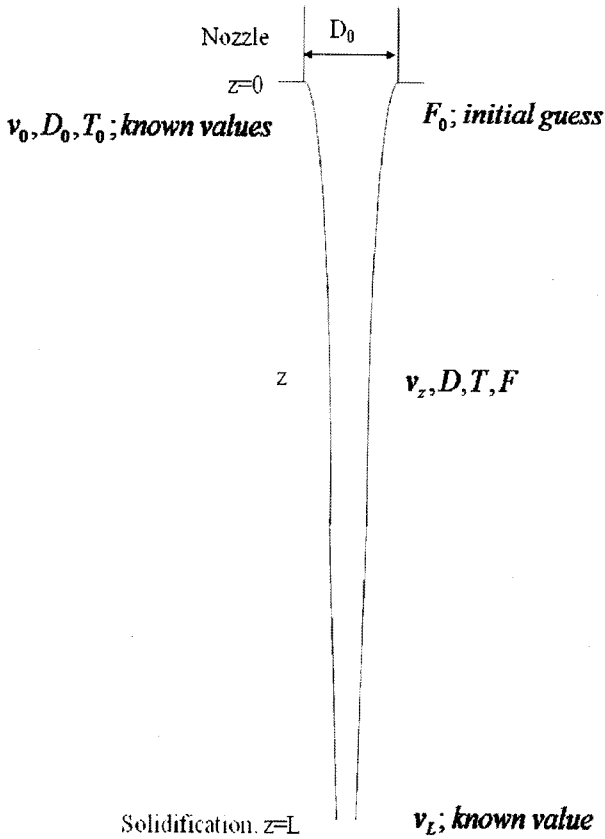


Fig. 1. Schematic of melt spinning process.

where η is the elongational viscosity.

The UCM model is selected as a viscoelastic constitutive equation. Two components of the UCM model are as follows (Kikutani, 1996)

$$\tau_{zz} + \lambda [v_z (d\tau_{zz}/dz) - 2\tau_{zz} (dv_z/dz) - v_z \tau_{zz} (d \ln T/dz)] = 2\mu (dv_z/dz), \quad (5)$$

$$\tau_{rr} + \lambda [v_z (d\tau_{rr}/dz) + \tau_{rr} (dv_z/dz) - v_z \tau_{rr} (d \ln T/dz)] = -\mu (dv_z/dz), \quad (6)$$

where τ_{zz} is the axial stress, λ the relaxation time, μ the shear viscosity and τ_{rr} the radial stress.

Eqs. (5) and (6) can be simplified to the following form:

$$d\tau_{zz}/dz = (2\tau_{zz}/v + 2\eta/3\lambda v) (dv_z/dz) - \tau_{zz}/\lambda v \tau_{zz} (d \ln T/dz). \quad (7)$$

The elongational viscosity of PET was assumed to be only a function of temperature (Shimizu *et al.*, 1985).

$$\eta = 0.73 \exp\left(\frac{5300}{T+273}\right). \quad (8)$$

The above governing equations are coupled with a lack of one more single equation for obtaining solutions. Therefore, a shooting method was used with the initial guess of the force at the spinneret to fit the boundary conditions of spinning speed; an iterative method was also employed. The boundary conditions applied in the simulation are

Table 1. Material parameters

Parameters	Values
Thermal conductivity of air (k_a , g/cm ³ sec ³ .°C)	2.63×10 ³
Kinematic viscosity of air (μ_a , cm ² /sec)	0.29
Specific heat capacity of PET (C_p , cm ² /sec ² .°C)	(0.3+6.0×10 ⁻⁴ T) ×4.2×10 ⁷
Density of PET (ρ , g/cm ³)	1.356-5×10 ⁻⁴ T

expressed as follows:

$$T(0) = T_{die}, v_z(0) = v_0, v_z(L) = v_L, \quad (9)$$

where T_{die} is the spinning temperature, v_0 the initial speed, v_L the spinning speed and L the distance from spinneret to winder. The dimension of the spinneret as the starting diameter in the simulation was used. Since the spinning process has a large length to diameter ratio, die swell effects could be neglected (George *et al.*, 1983). Several correlations for physical properties and transport coefficients are expressed below (Shimizu *et al.*, 1985).

$$h = 0.42 \left(\frac{k_a}{D}\right) Re_d^{0.334} \left[1 + \left(\frac{8v_a}{v_z}\right)^{2-0.1667}\right], \quad (10)$$

$$C_f = 0.37 Re_d^{-0.61}, \quad (11)$$

$$Re_d = \left(\frac{v_z D}{\mu_a}\right), \quad (12)$$

where k_a is the thermal conductivity of air, v_a the quench air velocity, μ_a the kinematic viscosity of air and Re_d the Reynolds number.

Some material parameters are summarized in Table 1 (Shimizu *et al.*, 1985). Gregory (1973) calculated relaxation times as a function of temperature and molecular weight for the viscoelastic response of molten PET given

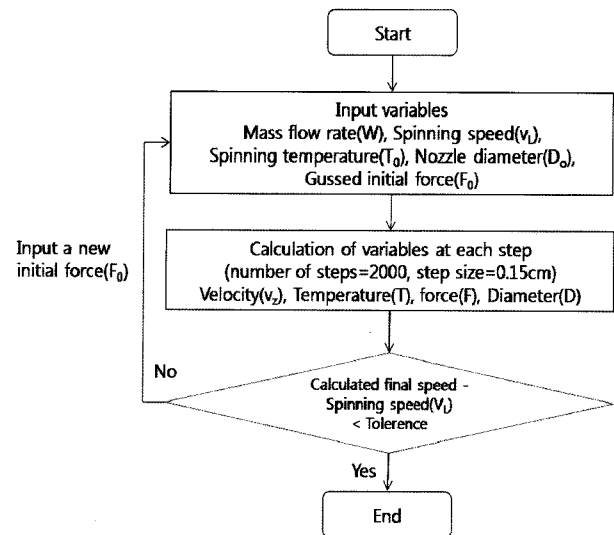


Fig. 2. Flow chart of the simulation.

Table 2. Spinning conditions in the simulation

No.	Mass flow rate (g/min-hole)	Spinning temperature (°C)	Spinning speed (m/min)
1	5.3	295	3000
2	5.3	295	5000
2	5.3	295	6000

in Eq. (13). The molecular weight effect was expressed by means of intrinsic viscosity.

$$\lambda = \frac{\exp\left(-11.9755 + \frac{6802.1}{T+273}\right) \times \left(\frac{IV}{4.68 \times 10^{-4}}\right)^{\frac{3.5}{0.68}}}{8.54 \times 10^{18}} \quad (13)$$

where *IV* is the intrinsic viscosity of polymer. Here, the *IV* was 0.63.

The Euler method was used to solve the asymptotic equation describing the dynamics of melt spinning. Fig. 2 shows a flow chart of the simulation. The step size was 0.15 cm with a tolerance of 0.001. The simulation program was made using FORTRAN. Spinning conditions are presented in Table 2.

3. Results and Discussion

Fig. 3 shows the calculated velocity profiles with a difference between the Newtonian and UCM models. The velocity profile of the running filament in the spinline shows a sigmoid form in the Newtonian model. The velocity of the UCM model was slower than that of the Newtonian model. The velocity build-up of the two models showed a similar trend near the spinneret. After an axial distance of 40 cm, the speed of the Newtonian increased

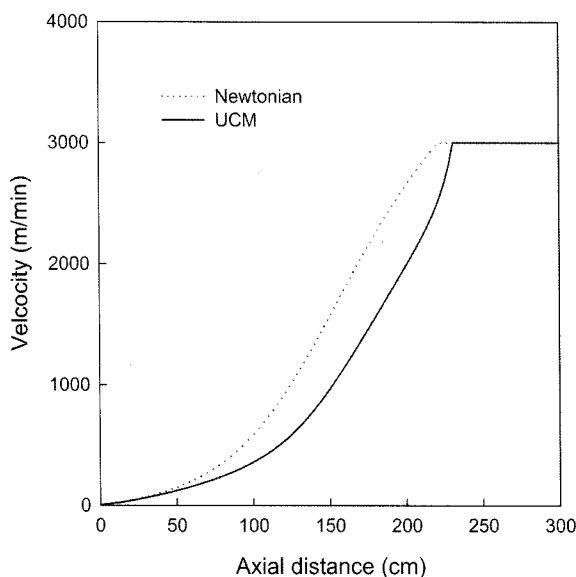


Fig. 3. Simulated velocity profiles along the spinline for different constitutive equations at the take-up speed of 3000 m/min.

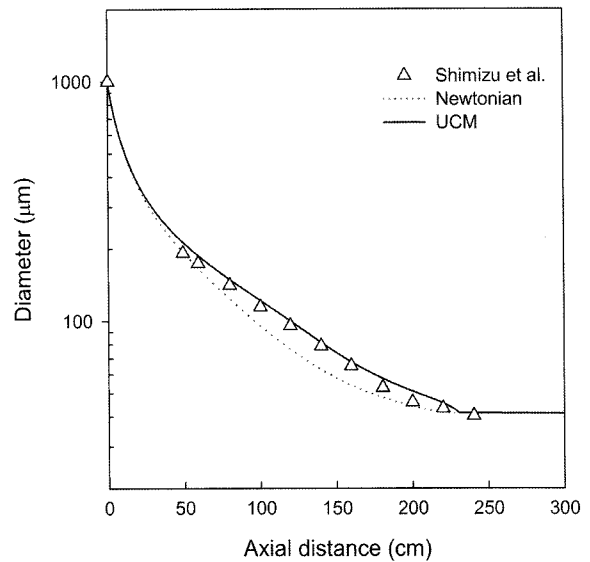


Fig. 4. Diameter profiles along the spinline for different constitutive equations at the take-up speed of 3000 m/min.

more than the UCM. A simple Maxwell model that assumed a constant modulus has also been reported (Shimizu *et al.*, 1985). In that spinning simulation, deformation continued after solidification and was difficult to affect in a real situation.

Fig. 4 shows diameter profiles along the spinline. Here, the previous experimental data obtained by Shimizu *et al.* (1985) are also shown. The diameter decreased exponentially in the spinline with the two models, showing similar profiles near the spinneret. A more rapid decrease, however, occurred in the Newtonian model at an axial distance of 25 cm. As shown in Fig. 3, the faster velocity increase

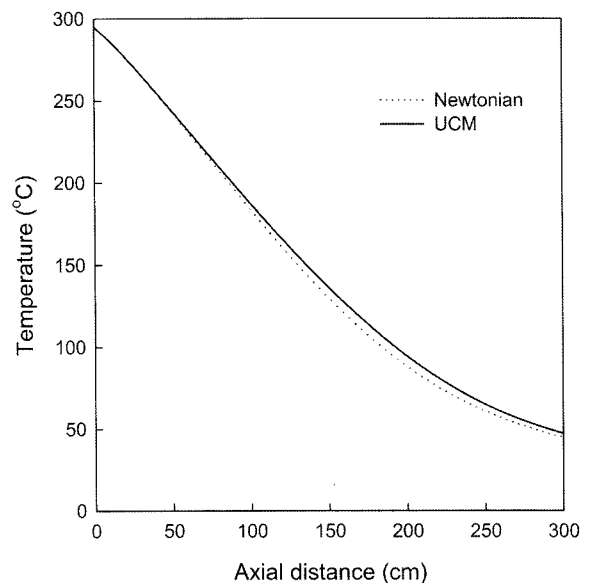


Fig. 5. Simulated temperature profiles along the spinline for different constitutive equations at the take-up speed of 3000 m/min.

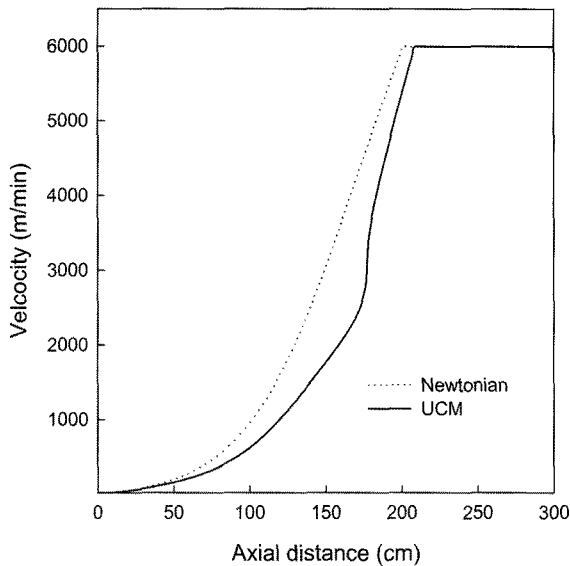


Fig. 6. Simulated velocity profiles along the spinline for different constitutive equations at the take-up speed of 6000 m/min.

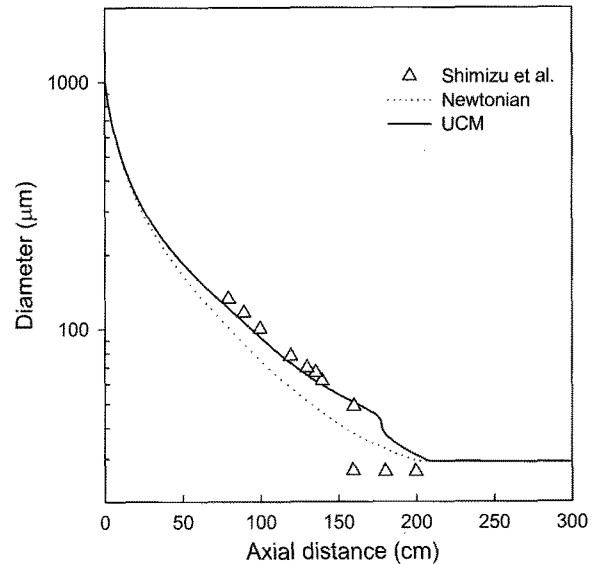


Fig. 7. Diameter profiles along the spinline for different constitutive equations at the take-up speed of 6000 m/min.

in the spinline of the Newtonian model gave rise to a rapid decrease in the diameter. Conversely, a smooth increase in velocity in the UCM model gave rise to a gentle decrease in diameter. As shown in Fig. 4, the UCM model fit better than the Newtonian, especially considering that viscoelasticity was important to simulate the melt spinning process more accurately.

Fig. 5 shows the temperature profiles at a spinning speed of 3000 m/min. The Newtonian molten polymer solidified slightly faster. The difference between the Newtonian and UCM was relatively small as heat transfer was affected mainly by the quench air temperature and velocity, both of which were fixed in the simulation.

Fig. 6 shows the velocity profiles for a high spinning speed of 6000 m/min. A spinning speed over 5000 m/min is known as a high speed spinning in PET spinning. At a spinning speed of 3000 m/min, the velocity build-up of the Newtonian model is faster than the UCM, considering that viscoelasticity delays velocity build-up in the UCM model. There is a characteristic high-speed spinning velocity build-up in the UCM model as an abrupt change in velocity at the intermediate axial position was observed.

Fig. 7 shows the diameter profiles for high-speed spinning. As in the case of 3000 m/min, the UCM model better fit the experimental data up until the position of the neck-like deformation, obtained by Shimizu *et al.* (1985). Nevertheless, the simulated values did not fit the neck-like deformation observed in high-speed spinning. In PET melt spinning, the neck-like deformation is a unique characteristic in high-speed melt spinning over 5000 m/min. In the UCM model, neck-like deformation was observed due to an abrupt increase in velocity shown in Fig. 6. However, the position and extent of the neck-like deformation were

not accurately predicted through only consideration of the viscoelastic constitutive equation. The Newtonian model diameter profiles showed exponential decrease irrespective of spinning speed, with no neck-like deformation. However, the neck-like deformation was observed in the UCM model. To simulate this deformation, further consideration on the neck criteria, such as stress-induced exothermic crystallization, should be implied in the governing equation.

Fig. 8 shows the velocity gradient for different spinning speeds. The maximum velocity gradient ranged from 106 to 1134 s^{-1} with spinning speed. Very sharp peaks in the

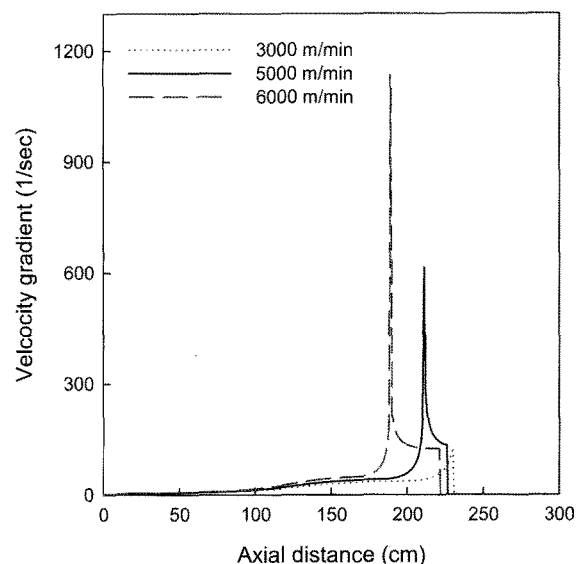


Fig. 8. Calculated velocity gradient along the spinline for different take-up speeds.

UCM model gave rise to neck-like deformations known to start at a spinning speed over 5000 m/min. Most research on neck-like deformation simulations use Newtonian constitutive equations with constraint conditions given to reveal neck-like deformations (Katayama and Yoon, 1985). However, they cannot predict the exact position of the neck-like deformation. Even though the prediction of the exact deformation position failed, applying the viscoelastic constitutive equation was necessary for simulating the high-speed spinning process as there is no neck-like deformation when using the Newtonian model. If neck criteria are involved in the simulation, the exact position of the neck-like deformation would be predicted.

4. Conclusion

Numerical simulations of the melt spinning process for different constitutive equations were carried out and compared with each other. The UCM model fit the diameter profile well, considering the relaxation time gave rise to more accurate predictions in melt spinning. The Newtonian showed slight deviations from the experiment along the spinline. In high-speed spinning, the UCM model showed neck-like deformations not observed in the Newtonian. Regardless, in high-speed spinning, the UCM model could not fit the accurate position of the neck-like deformation.

Acknowledgements

This research was supported by the Yeungnam University research grants in 2008.

References

- Cao, J., T. Kikutani, A. Takaku and J. Shimizu, 1989, Nonisothermal orientation-induced crystallization in melt spinning of polypropylene, *J Appl Polym Sci.* **37**, 2683-2697.
- Denton, J. S., J. A. Cuculo and P. A. Tucker, 1995, Computer simulation of high-speed spinning of PET, *J Appl Polym Sci.* **57**, 939-951.
- Goerge, H. H., 1982, Model of steady-state melt spinning at intermediate take-up speed, *Polym Eng Sci.* **22**, 292-299.
- George, H. H., A. Holt and A. Buckley, 1983, A study of structural development in high speed spinning of poly(ethylene terephthalate), *Polym Eng Sci.* **23**, 95-99.
- Gregory, D. R., 1973, Departure from Newtonian Behavior of Molten Poly(ethylene terephthalate), *Transactions of Soc. Rheology* **17**, 191-195.
- Katayama, K., and M. G. Yoon, 1985, High-speed fiber spinning, Wiley-Interscience, New York, 207-223.
- Kase, S. and T. Matsuo, 1965, Studies on melt spinning. I. Fundamental equations on the dynamics of melt spinning, *J Polym Sci, Polym. Chem.* **3**, 2541-2554.
- Kikutani, T., J. Radhakrishnan, S. Arikawa, A. Takaku, N. Okui, X. Jin, F. Niwa and Y. Kudo, 1996, High-speed melt spinning of bicomponent fibers: Mechanism of fiber structure development in poly(ethylene terephthalate)/polypropylene system, *J Appl Polym Sci.* **62**, 1913-1924.
- Shimizu, J., N. Okui and T. Kikutani, 1985, High-speed fiber spinning, Wiley-Interscience, New York, 173-201.

Appendix

Eq. (5) minus Eq. (6) yields

$$\begin{aligned} & \tau_{zz} + \lambda [v_z(d\tau_{zz}/dz) - \tau_{zz}(dv_z/dz) - 3\tau_{zz}(dv_z/dz) - v_z\tau_{zz}(d\ln T/dz)] \\ & - \{ \tau_{rr} + \lambda [v_z(d\tau_{rr}/dz) - \tau_{rr}(dv_z/dz) - v_z\tau_{rr}(d\ln T/dz)] \} \\ & = 2\mu(dv_z/dz) - (-\mu(dv_z/dz)), \end{aligned} \quad (\text{A.1})$$

Eq. (A.1) rewritten as:

$$\begin{aligned} & (\tau_{zz} - \tau_{rr}) + \lambda \left[v_z(d(\tau_{zz} - \tau_{rr})/dz) + (\tau_{zz} - \tau_{rr})(dv_z/dz) \right] \\ & \left[-3\tau_{zz}(dv_z/dz) - v_z(\tau_{zz} - \tau_{rr})(d\ln T/dz) \right] \\ & = 3\mu(dv_z/dz) = \eta(dv_z/dz). \end{aligned} \quad (\text{A.2})$$

where $\tau_{zz} - \tau_{rr}$ is given by:

$$\tau_{zz} - \tau_{rr} = F/A. \quad (\text{A.3})$$

Then, Eq. (A.3) can be written as:

$$\begin{aligned} & F/A + \lambda \left[v_z(d(F/A)/dz) + F/A(dv_z/dz) - 3\tau_{zz}(dv_z/dz) \right] \\ & \left[-v_z(F/A)(d\ln T/dz) \right] \\ & = \eta(dv_z/dz). \end{aligned} \quad (\text{A.4})$$

To derive Eq. (A.4), the following relations are used:

$$d(F/A)/dz = (1/A)d(F)/dz + Fd(1/A)/dz, \quad (\text{A.5})$$

$$d(1/A)/dz = (-1/A^2)(dA/dz), \quad (\text{A.6})$$

$$(dA/dz) = (-A/v_z)(dv_z/dz). \quad (\text{A.7})$$

$$\begin{aligned} d(F/A)/dz &= (1/A)d(F)/dz + Fd(1/A)/dz = (1/A)d(F)/dz + \\ & F(-1/A^2)(dA/dz) = (1/A)d(F)/dz + (F/Av_z)(dv_z/dz) \end{aligned} \quad (\text{A.8})$$

Eq. (A.4) can be simplified as:

$$\begin{aligned} & F/A + \lambda \left[v_z \{ (1/A)d(F)/dz + (F/Av_z)(dv_z/dz) \} + \right. \\ & \left. (F/A)(dv_z/dz) - 3\tau_{zz}(dv_z/dz) - v_z(F/A)(d\ln T/dz) \right] \\ & = \eta(dv_z/dz) \end{aligned} \quad (\text{A.9})$$

$$\begin{aligned} & F/A + \lambda \left[v_z \{ (1/A)d(F)/dz + (F/Av_z)(dv_z/dz) \} + \right. \\ & \left. (F/A)(dv_z/dz) - 3\tau_{zz}(dv_z/dz) - v_z(F/A)(d\ln T/dz) \right] \\ & = \eta(dv_z/dz) \end{aligned} \quad (\text{A.10})$$

A/λ is multiplied on both sides of Eq. (A.10) to yield:

$$\begin{aligned} & (\eta A/\lambda + 3A\tau_{zz} - 2F)(dv_z/dz) \\ & = v_z(dF/dz) + F/\lambda - Fv_z(d\ln T/dz). \end{aligned} \quad (\text{A.11})$$